

Water Jet Impingement Cooling System for Evaluation of Microstructural Phase Transformation of Hot Steel Plates

T.O. Onah^{1*}, A.O. Odukwè² and J. N. Ani³

¹Department of Mechanical and Production Engineering, Enugu State University of Science and Technology Enugu, Enugu Nigeria

²Department of Mechanical Engineering, University of Nigeria, Nsukka

³Department of Mechanical and Production Engineering, Enugu State University of Science and Technology Enugu, Nigeria

Original Research Article

*Corresponding author

T.O. Onah

Article History

Received: 02.04.2018

Accepted: 10.04.2018

Published: 30.04.2018

DOI:

10.36347/sjet.2018.v06i04.004



Abstract: Cooling of the steel on the run-out table system was done through impingement water jets on the top of hot steel plates to study microstructural phase transformation of the final product and its hardness. Controlled accelerated cooling system was designed and developed for this target in order to achieve the desired mechanical properties of the final steel products. In order to achieve this goal, the microstructural and hardness test of the workpiece before and after was conducted. The examinations of microstructural phase transformation of pipe diameters, D, of 20mm, 25mm, 32mm and 45mm, and impingement gaps, H, of 40mm and 70mm from austenite temperature of 920°C and exposed to surface temperatures of 438°C and 470°C were investigated. The cooling was controlled at 200°C. The control sample had 39.9 hardness number before heating. However, after heating and impingement cooling, the examinations revealed hardened phase transformed needles of marenstitie with hardness number 59.5 from control of 39.9, for pipe diameter, D, of 20mm and H = 70mm. Moreover, the examinations also revealed hardened phase transformed needles of martensite with hardness number 70 from control of 39.9, for pipe diameter, D, of 45mm and, H, of 70mm. The results suggested that better advanced steel grades occurred with marenstitic phase with hardness number 59.5 that fell within RHN range.

Keywords: Hot steel plate, impingement pilot plant run-out table system, temperature, hardness number, microstructure, impingement gap, pipe diameter.

INTRODUCTION

The intensity of cooling employed in thermo-mechanical controlled process (TMCP) affect the microstructural evolution process such as austenite

decomposition and precipitation. Different cooling paths of the steel on run-out table lead to different phase transformation such as ferrite, pearlite, bainite, and/or martensite as shown in fig. 1.

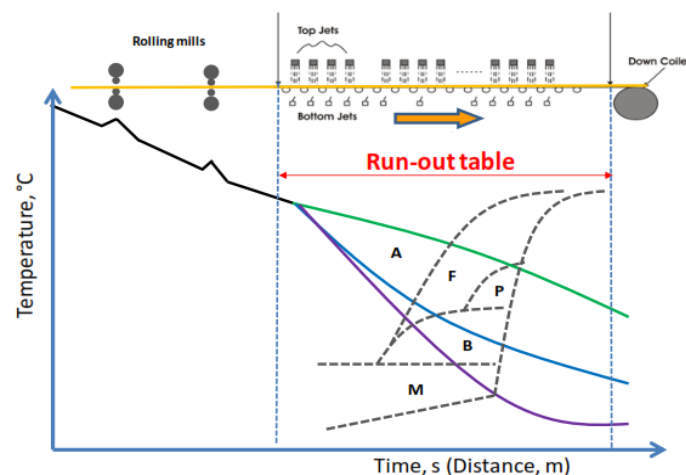


Fig-1: Schematic of hot rolling mill of steel plates and strips. The schematic plot shows temperature variation versus time and its effect on the phase transformation of austenite decomposition. A: austenite, F: ferrite, P: pearlite, B: bainite, M: martensite.

pearlite B: bainite, M: martensite

Role of Microstructure

In steel and cast irons, the microstructural constituents have the names ferrite, pearlite, bainite, martensite, cementite and austenite. In most all other metallic systems, the constituents are not named, but are simply referred to by a Greek letter (α , β , γ etc.) derived from location of the constituent on the other hand have been widely studied by [1].

It can be seen that the four examples described above have very different microstructures, the structural steel has a ferrite plus pearlite microstructure; the rail steel has a ferrite plus pearlite microstructure; the machine housing (lathe) has a ferrite plus pearlite matrix with graphite flakes and the jaw crusher microstructure contains marten site and cementite [2].

In each case, the microstructure plays the primary role in providing the properties desired for each application in phase transformation. From this example, one can see how materials properties can be tailored by microstructural manipulation or alteration. Knowledge about microstructure is thus paramount in component design and alloy development.

Ferrite

A wide variety of steels and cast iron fully exploit the properties of ferrite. However only a few commercial steels are completely ferrite. An example of the microstructure of a fully ferrite, ultralow carbon steel is shown in fig.2. Ferrite is essentially a solid solution of iron containing carbon or one or more alloying elements such as silicon, chromium manganese and nickel. There are two types of solid solutions interstitial and substitutional.

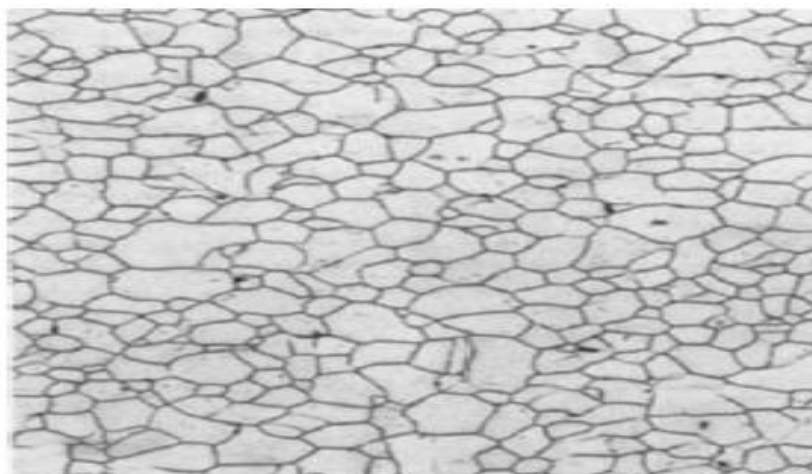


Fig-2: Microstructure of fully ferrite of low carbon steel [3]

Ferrite is essentially a solid solution of iron containing carbon or one or more alloying elements such as silicon, chromium manganese and nickel. There are two types of solid solutions interstitial and substitutional. In an interstitial solid solution elements with small atomic diameter for example, carbon and nitrogen, occupy specific interstitial sites in the body centered cubic (Bcc) iron crystalline lattice. These sites are essentially the open spaces between the large iron atoms. In a substitutional solid solution, elements of

similar atomic diameter are replaced or substitute for iron atoms.

Pearlite

As the carbon content of steel is increased beyond the solubility limit (0.02% C) on the iron carbon binary phase diagram fig.3, a constituent called pearlite forms. Pearlite formed by cooling the steel through the eutectoid temperature (the temperature of 727⁰C by the following reaction.



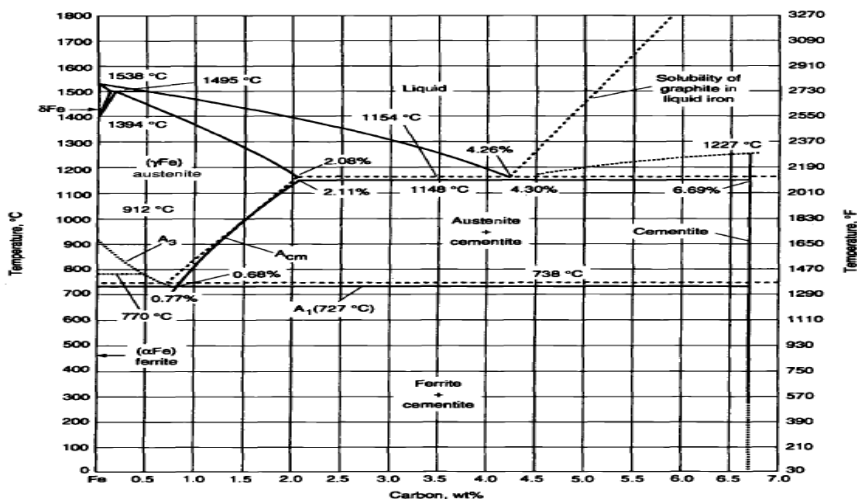


Fig-3: Iron carbon binary phase diagram [4]

A fully pearlite microstructure is formed at the eutectoid composition of 0.78% C. as can be seen in figs.4 and 5, pearlite forms as colonies where the

lamellae are aligned in the same orientation. The properties of fully pearlite steels are determined by the spacing between the ferrite – cementite lamellae.

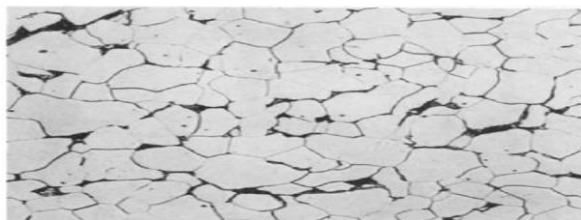


Fig-4: Micrograph of pearlite in low carbon steel 1000x [5]

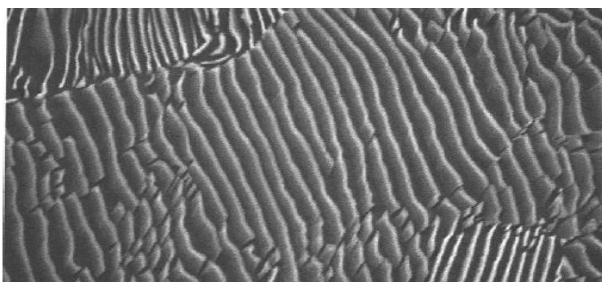


Fig- 5: Micrograph of pearlite showing ferrite and cementite 10,000x [5]

Marten site

Marten site is essential a supersaturated solid solution of carbon in iron. The amount of carbon in marten site far exceeds that that found in solid solution in ferrite. Because of this, the normal body centered cubic (bcc) lattice is distorted in order to accommodate the carbon atoms. The distorted lattice becomes body-centered tetragonal (bet). In plain carbon and low alloy steels, this supper saturation is generally produced through very rapid cooling from the austenite phase region (quenching in water, feed-water, brine, feed brine, oil or aqueous polymer solution) to avoid forming ferrite, pearlite and kainite. Some highly alloyed steels can form marten site upon air cooling.

Depending on carbon content, marten site in its quenched state can be very hard and brittle and because of this brittleness, marten site steels are usually tempered to restore some ductility and increase toughness.

A continuous cooling transformation (CCT) fig.5 diagram for type 4340 is shown in fig.6, indicates that marten site forms at cooling rates exceeding about 1000⁰C/min. most commercial martensitic steels contain deliberate alloying additions intended to suppress the formation of other constituents that is ferrite, pearlite and kainite – during continuous cooling. This means that these constituents form at slower

cooling rates, allowing martensite to form at the faster cooling rates, for examples, during oil and water quenching. This concept is called hardenability and is essentially the capacity that leads to microstructural phase transformation of steel to generate a needle like-hardened martensite structure fig.7.

This research tries at providing a predictive tool in order to control more accurately the temperature profile on the run-out table and thus improve the mechanical and metallurgical properties of the steel product hitherto achievable only by alloying, which is relatively expensive.

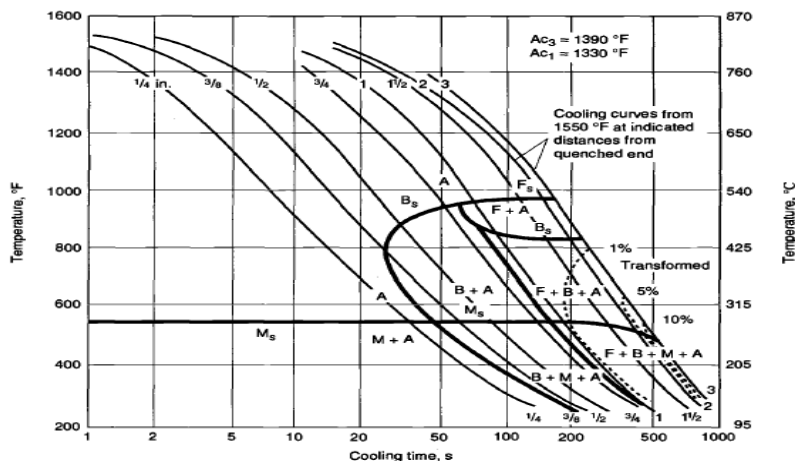


Fig-6: The CCT Diagram for type 4340 Steel Austenitized at 845⁰C [3]

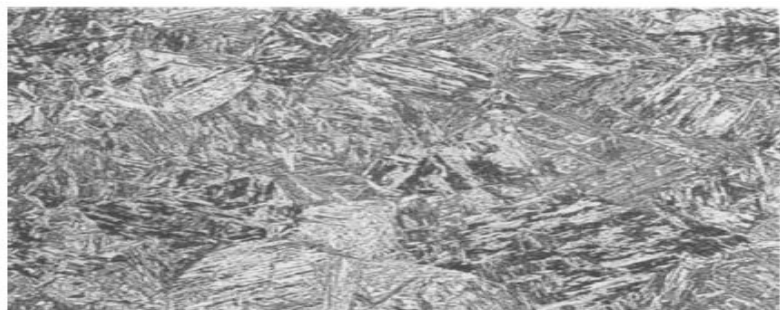


Fig-7: Microstructure of a typical martensite at 200x [6]

MATERIALS AND METHODOLOGY

Experimental Set –Up For Pilot Scale Plant Run Out Table

A pilot scale run out table (ROT) system was designed and constructed in Mechanical and Metallurgical Engineering Foundry Laboratory (MMEFL), ESUT. A schematic diagram of the run-out table and picture of the set-up in fig.8

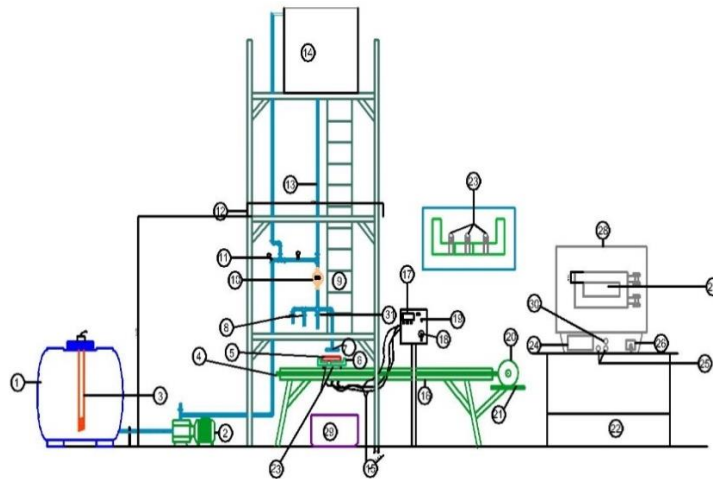


Fig-8: Schematic diagram of pilot plant for this research in MMEFL

- Water tank, 2. Electric pump, 3.Heater, 4.Conveyor screw, 5.Work piece, 6.Work piece bed, 7.Impingement nozzle, 8.Ball gauge socket, 9.Ladder, 10.Flow meter, 11.Pressure meter, 12.Tower, 13.PVC pipe, 14.Reservoir, 15.Thermocouple wire, 16.Motorized Screw conveyor, 17.Thermocouple control panel, 18.Regulator, 19.Lock, 20.Electric motor, 21.Electric motor support, 22.Furnace support, 23.Thermocouple, 24.Furnace indicator, 25.Furnace switch, 26.Furnace regulator, 27.Furnace door, 28.Electric furnace, 29.Water collector, 30.Pilot light Header.

electric heater of 9kw of 330volts was situated in the tank and was used to adjust the temperature of water between 10-70°C .The water temperatures readings were taken by mercury in bulb thermometer.

In this study, one type of nozzle was used; planar (water or curtain) nozzle. The cross section is 12x 12 mm of 30 × 90mm with 0.8 mm with 30 number holes of jet diameter. A control panel mounted on a stand was used to read the surface temperatures of steel before and after the impingement. It has a red icons buttons that controls and records the temperature variations with digital read out on a steel cased panel.

The system has been designed to simulate industrial cooling condition for run-out table cooling of stationary plates in hot strip and plate mills [7]. It enables heat transfer to be studied during cooling of stationary plates. In this study heating was provided by an electric furnace where a steel plate was heated up to a temperature of 920°C in Metallurgical and Material Laboratory ESUT Enugu, Nigeria. Fusing a motorized ASYNCHRONOUS ROTOR gear powered conveyor drive system of 0.75kw of 1500rpm to operate a gear of 1:24 by ratio with 50HZ under an ac. of 240volts; the steel plates were transported from the furnace to the cooling tower for the stationary experiments.

The cooling system features a closed water loop where 0.945m³ (945 liters) of water was circulated throughout the experiment through the cooling jet nozzles. Surface temperatures, water temperatures, impingement heights or nozzle-to- surface spacing (impingement height) and flow rates were controlled. An ATLAS (ATP 60) water pump that provided total water flow rates of 60L/min was employed. It pumped water to the impingement plate from the water tank below to the target plate through the flow meter, nozzle header via impingement jet nozzle to the hot plate. An

Experimental procedure

After the required temperature of 920°C was reached in the electric furnace, the workpiece was removed and kept on the motorized screwed conveyor that transported the plate towards the cooling jet impingement target. For the experiment, the center of the plate was positioned under the jet nozzle, and the water flow from tank was started. The water header was positioned for different flow of water using different water pipe diameters and heights. The pressure gauge and flow meter were also opened to read the values of pressure and flow rate with stop watch. However, the initial surface temperatures of the plate (Ti) at the onset of water impingement cooling varied from 450 to 550°C. Temperature data of various thermocouple locations were collected when the surface temperature drops below 3°C of the three thermocouples and average initial or surface temperature was recorded. When the controlled impingement cooling reached 200°C, 180°C, 160°C and 300°C, 280°C and 260°C respectively, the flow was stopped using stop watch. The evaporated water was gotten, by subtracting volume of water collected from volume of water used, using flow meter and measuring cylinder.

Microstructural Test Apparatus

Table-1: Chemical Composition of Test low Carbon Steel Plate (LCS)

Steel chemical composition	Fe	C	Si	Mn	S	P	Cr	Ni	Mo	Cu
Wt. %	98.480	0.25	0.095	0.755	0.042	0.010	0.053	0.051	0.016	0.103
Steel chemical composition	Al	V	Co	Sn	As	Nb	Pb	W	B	
Wt. %	0.008	0.011	0.011	0.0377	0.010	0.000	0.000	0.050	0.0001	

The microstructural test of the specimens was carried out with an optical microscope of (fig. 9) at the Metallurgical and Material Engineering Laboratory

(MMEL), ESUT, Agbani. The tests were under with the optical microscopic examination of 100µm at 100X magnification.

KEYS

1. Revolving nosepiece
2. Medium power Objective lens
3. High power objective lens
4. Body tube
5. Lower power objective lens
6. Stage clip
7. Stage
8. Iris diaphragm
9. Projection lens
10. Base
11. Ocular lens
12. Arm
13. Fine focus
14. Coarse focus
15. Power switch

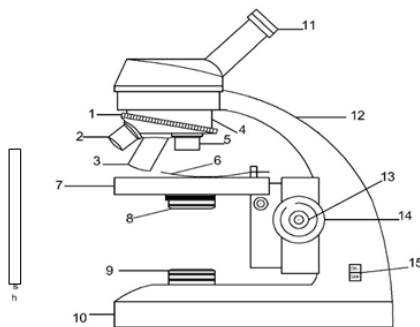


Fig-9: Optical microscope

Initial Microstructural Test

The microstructure of fig 10 shows the internal composition of the workpiece before heating and impingement.

Fig. 10 shows an iron –carbon (98.480Fe - 0.25C) control sample of optical micrograph of a mixed

microstructure of bainite and marten site in low carbon steel. The bainite etched dark because it is a mixture of ferrite and cementite. The residual phase is untampered marten site which etches lighter because of the absence of carbide precipitates. The presence of darker spot of pearlite indicates that the sample is a hypo eutectoid steel, between 0.008 to 0.76 wt%C [8].

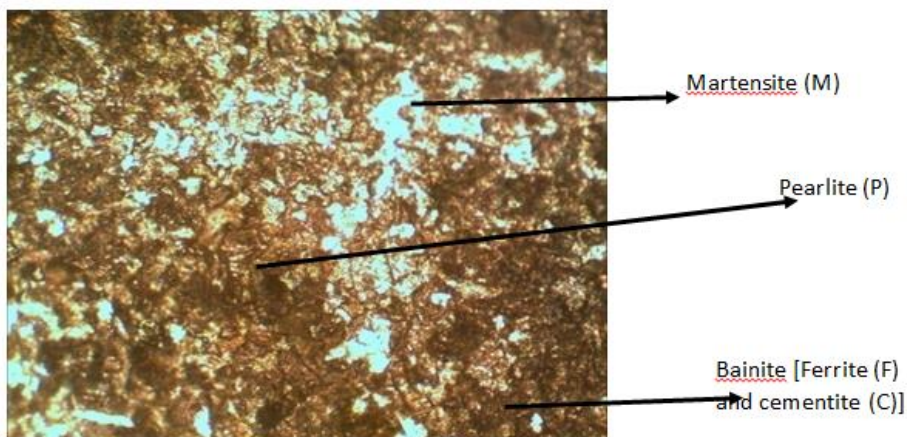


Fig-10: Microstructure of workpiece before heating and impingement, 100 x magnifications

Initial Hardness Test

The hardness tests were carried out with a digital display Rockwell harness tester fig.11 at the Metallurgical and Material Engineering Laboratory (MMEL), ESUT, Agbani. The depth of penetration of

an indenter (diamond), under a large 10kg load was used to determine the penetrations. The hardness number of the workpieces before heating and water jet impingement cooling was found to be 38.9.

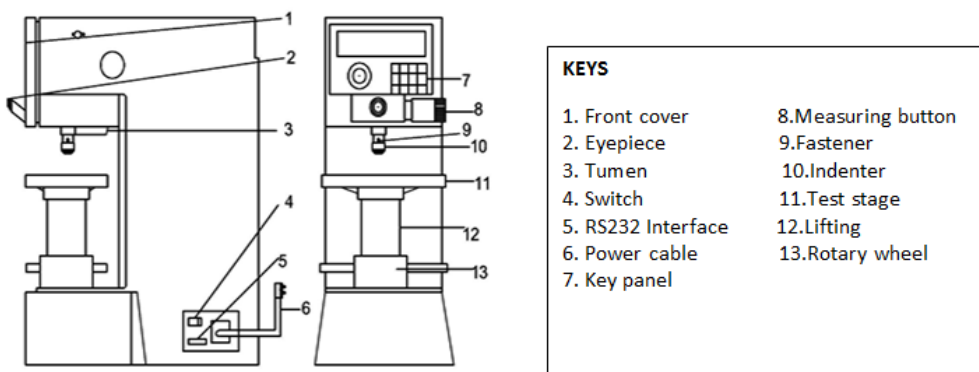


Fig-11: Rockwell Hardne Test Machine

RESULTS AND DISCUSSION

Microstructural Phase Transformation of the Micrographs after Heating and Impingement Cooling

The micrographs of figs.12 a, b, c and d, and figs.13 a, b, c and d respectively, depict the microstructural phase transformation from austenite temperature of 920°C through water jet impingement cooling of range 438 to 500°C, to a hardened needle like martensitic forms via ferrite and pearlite. The phase change of marten site occurred when cooling rate from austenite was sufficiently fast in the different

impingement gaps of H = 40mm and 70mm at different pipe diameters of D= 20mm, 25mm, 32mm and 45mm . It is a hard constituent phase transformation due to the carbon which was trapped in the workpiece during impingement cooling .The temperature range of martensitic phase transformation occurred between 500°C to below room temperature that depended on the hardenability of the specimen from the Rockwell Hardness test carried out. The marten site start temperature (M_s) to marten site finish temperature (M_f) is typically of the order of 1500C to 300°C [7]; $M_s = 500$ to 300°C- 35Mn – 20Cr and 15Ni.

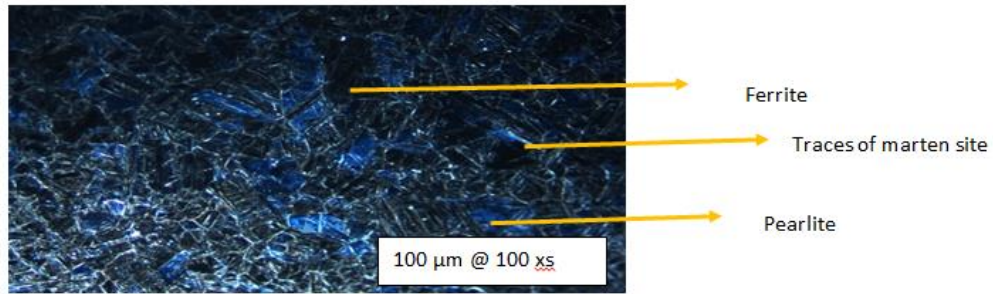


Fig-12a: Sample of D= 20mm, H= 70mm @ surface temperature 469⁰C

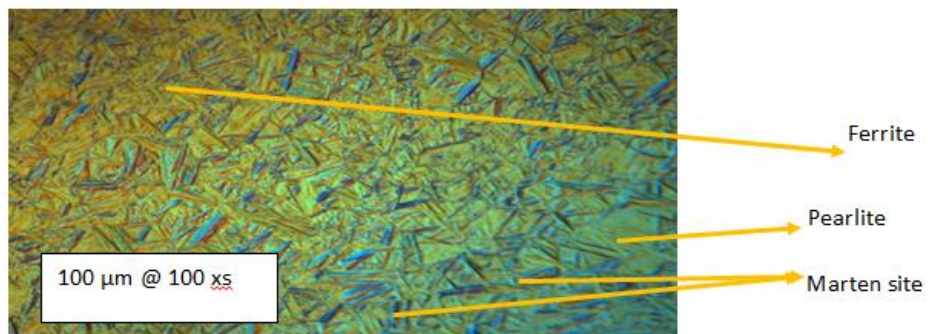


Fig-12b: Sample of D= 25mm, H= 70mm @ surface temperature 463⁰C

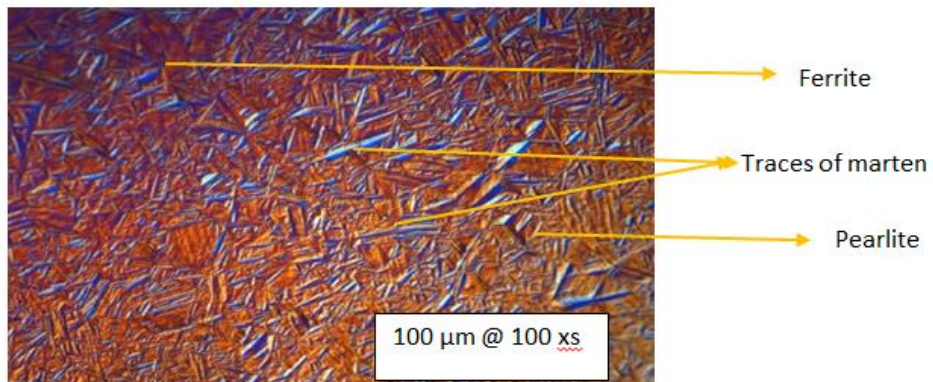


Fig-12c: Sample of D= 32mm, H= 70mm @ surface temperature 440⁰C

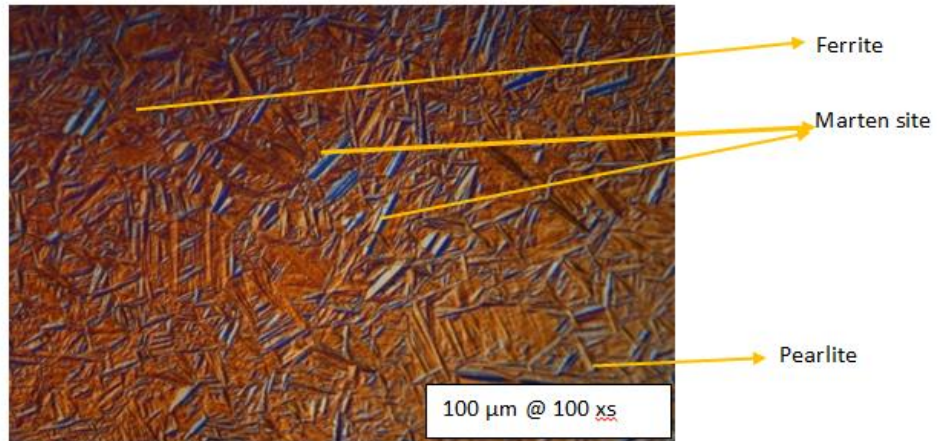


Fig-12d: Sample of D= 45mm, H= 70mm @ surface temperature 438⁰C

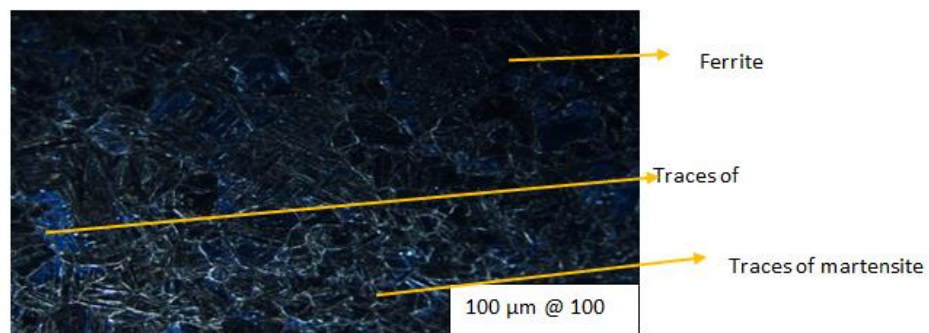


Fig-13a: Sample of D= 20mm and H= 40mm @ surface temperature 500⁰C

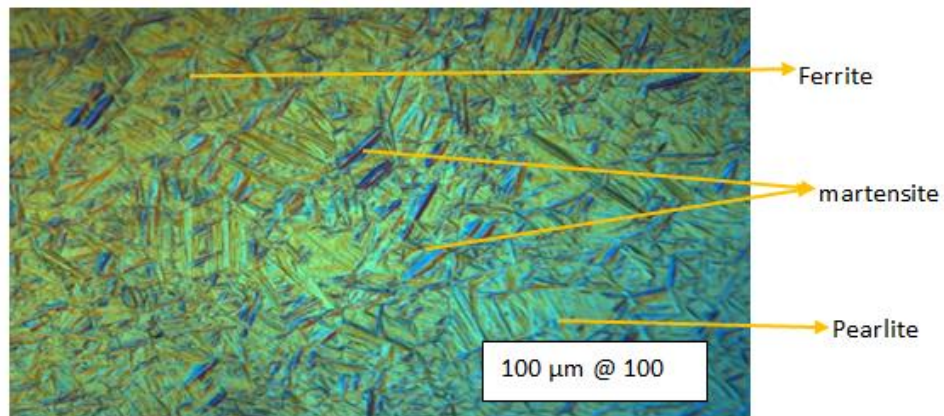


Fig-13b: Sample of D= 25mm, H= 40mm @ surface temperature 500⁰C

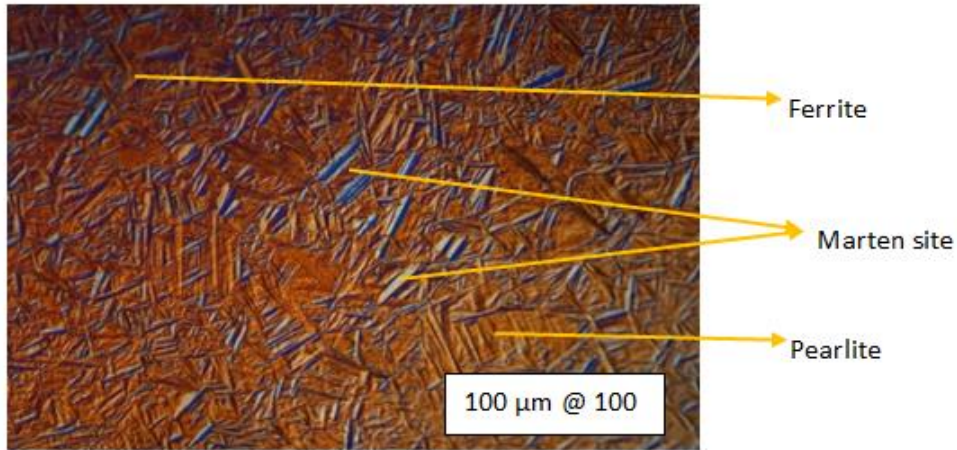


Fig-13c: Sample of D= 32mm, H= 40mm @ surface temperature 470⁰C

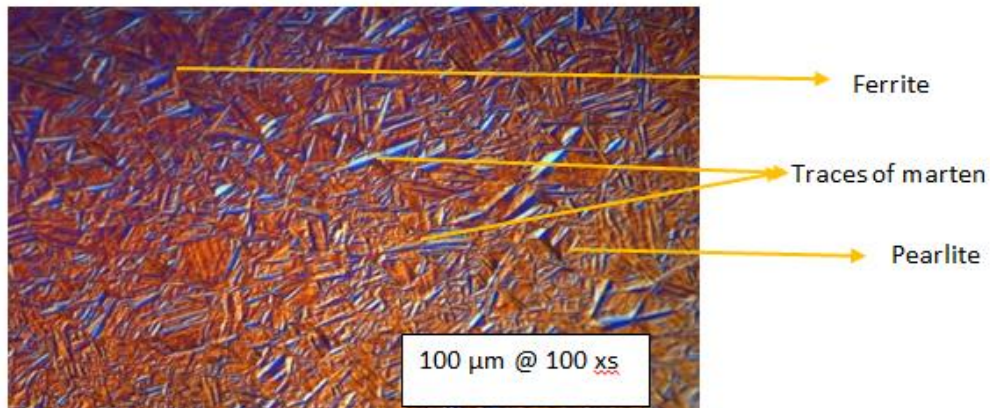


Fig-13d: Sample of D= 45mm, H= 40mm @ surface temperature 458⁰C

Hardness Samples Test

Table-2 : Rockwell Hardness Sample for Diameter of D=20mm,25mm,32mm and 45mm at Constant Height of H =70mm

RHT SAMPELS	Control RHN	Left RHN	Center RHN	Right RHN	Aérage Values RHN:LCR
D=20mm,H= 70mm @200 ⁰ C	38.9	50.1	59.5	50.4	53.33333333
D=25mm,H= 70mm @ 200 ⁰ C	38.9	45.4	58.6	45	56.4
D=32mm,H= 70mm @200 ⁰ C	38.9	45	57.9	45	54.23333333
D=45mm,H= 70mm @200 ⁰ C	38.9	44	55	44.3	48.73333333

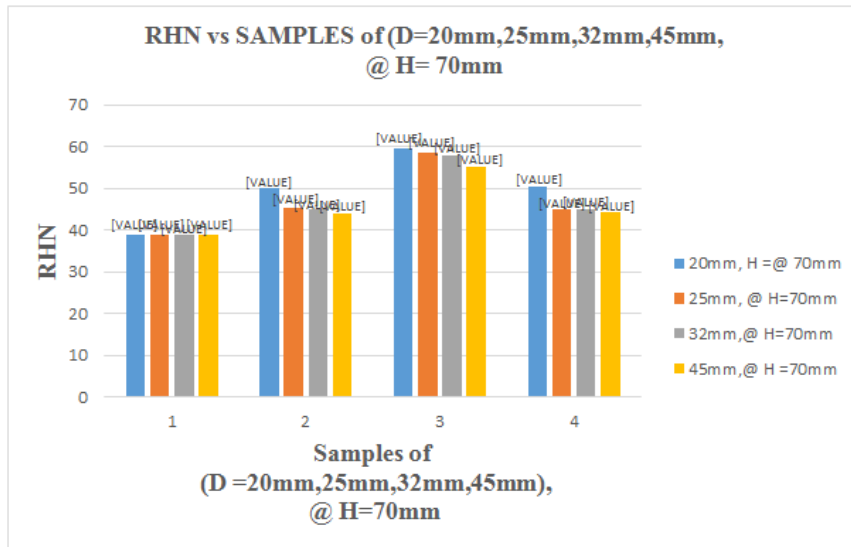


Fig-14a: Bar Charts of Comparative of D= 20mm, 25mm, 32mm and 45mm at impingement gap H =70mm

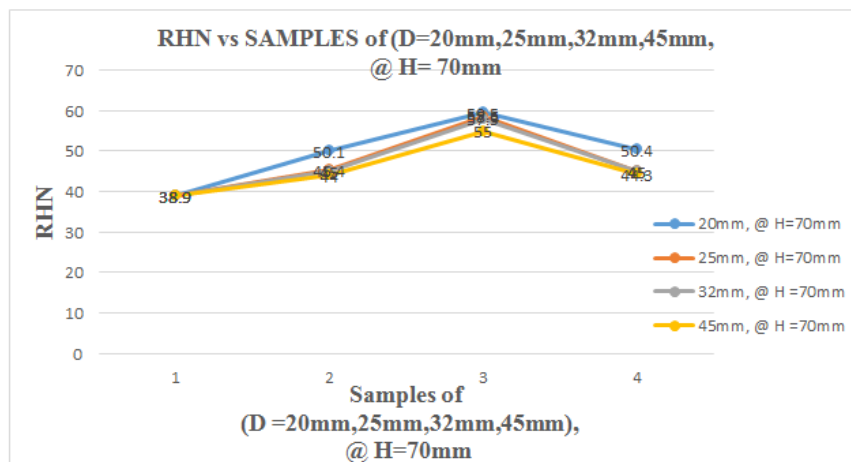


Fig-14b: Graphs of Comparative of D= 20mm, 25mm, 32mm and 45mm at impingement gap H =70mm

Figs.14a and 14b depict that with 20mm pipe diameter at the impingement gap H = 70mm, the hardness number is 59.5, followed by 32mm diameter of hardness number 58.6. Then with diameter 25mm the hardness is 57.9. However, the lowest hardness number 55 occurred at 20mm diameter. Moreover, the hardness decreases from smaller pipe diameter flow to bigger pipe diameter at H= 70mm.

The microstructure fig.12a, b, c and d show the grain transformation from austenite to martensitic

phase. Fig.12a with traces of martensite has least hardness number of 55. Figs.12b and c, show dark hardened martensitic formations from ferrite and pearlite with hardness numbers 57.9 and 58.6 figs.11a and b respectively. However, fig 12d shows fine clearer hardened transformed martensite, from austenite 9200C for 1hr, exposed to surface temperature of 438⁰C and cooled at 200⁰C. through ferrite and pearlite phases with highest hardness number of 59.5 which gives good advanced steel grades[9].

Table-3: Rockwell Hardness Sample for diameters 20mm, 25mm, 32mm and 45mm at a constant height 40mm

RHT SAMPELS	Control RHN	Left RHN	Center RHN	Right RHN	Average Values RHN:LCR
D=20mm, H= 40mm @ 200 ⁰ C	38.9	46.4	53	46	51.76666667
D=25mm, H= 40mm @ 200 ⁰ C	38.9	48	54.1	47.8	59.03333333
D=32mm, H= 40mm @ 200 ⁰ C	38.9	49.8	62.1	50	52.76666667
D=45mm, H= 40mm @ 200 ⁰ C	38.9	50.3	70	50	56.76666667

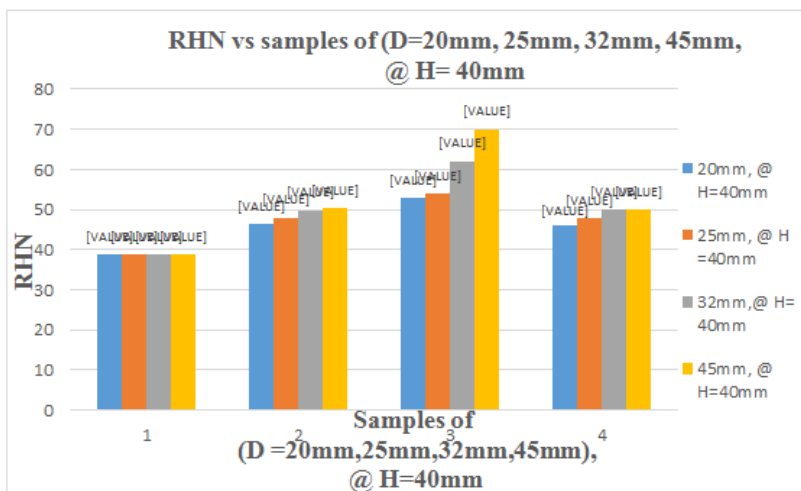


Fig-15a : Bar charts of comparative combinations of D= 20mm, 25mm, 32mm and 45mm at impingement gap H =40mm

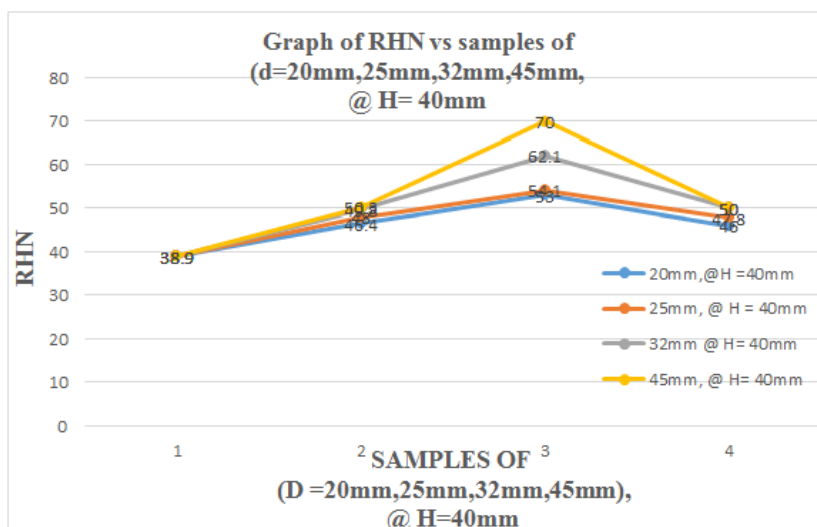


Fig-15b: Graphs of comparative combinations of D=20mm, 25mm, 32mm and 45mm at impingement gap H =40mm

Figs.15a and 15b depict that with 45mm pipe diameter at the impingement gap H = 40mm, the hardness number is 70 , followed by 32mm diameter of hardness number 62.1. Then with diameter 25mm the

hardness is 54.1. However, the lowest hardness number 53 occurred at 20mm diameter. The hardness increases from smaller pipe diameter flow to bigger pipe diameter at H= 40mm.

The microstructure fig.13a, b, c and d show the grain transformation from austenite to martensitic phase. Fig.13a with traces of martensite has least hardness number of 53. Figs.13b and c, show dark hardened martensitic formations from ferrite and pearlite with hardness numbers 54.1 and 62.1 figs.13a and b respectively[10, 11]. However, fig. 13d shows fine clearer hardened transformed martensite from austenite temperature of 920°C for 1hr, exposed to surface temperature of 470°C and cooled at 200°C, through ferrite and pearlite phases with highest

hardness number of 59.5 , also suggessting good advanced steel grades[9].

CONCLUSION

The examinations of microstructural phase transformation of pipe diameter D = 20mm and impingement gap H=70mm from austenite temperature of 920°C for 1hr , exposed to surface temperature of 438°C and cooled at 200°C, through ferrite and pearlite phases showed clearer needles of martensite with hardness number of 59.5. Also phase

transformation of pipe diameter $D = 45\text{mm}$ and impingement gap $H=40\text{mm}$ from austenite temperature of 920°C for 1hr, exposed to surface temperature of 470°C and cooled at 200°C , through ferrite and pearlite phases showed clearer needles of martensite with hardness number of 70.

However, the martensite phase with hardness number 59.5 of pipe diameter $D = 20\text{mm}$ and $H = 70\text{mm}$, that falls within the RHN [9] suggests better advanced steel grades when compared with the martensite phase with hardness number 70 of pipe diameter $D = 40\text{mm}$ and impingement gap 45mm .

REFERENCES

1. Honeycombe RWK. Teel- Microstructure and properties, American Society for Metal. 2012.
2. Hyzak JM and Berstern IM. Metal Trans A. 2010; Vol. 7A, P 1217
3. Krauss G. J Iron steel Inst. Jpn, int, 2015; Vol. 35 (No.4)., p34
4. Krauss G. Microstructures, Processing and properties of Steels, properties and Selection; Irons, Steels, and High-performance Alloys. 2009; Vol.1, ASM Handbook, p 20.
5. Pickering FB (2011). Towards improving toughness and Ductility Climax Molybdeum Co. p.
6. Microalloy 75. *Conference Proceedings Union Curtside Corp.* 2005, Oct.15th; p.5
7. Prodanovic V, Fraser D, Militzer M. Simulation of Runout Table Cooling by Water Jet Impingement on Moving Plates—A Novel Experimental Method. InProc. 2nd Int. Conf. on Thermomechanical Processing of Steel, Verlag Stahleisen 2004 Jul (pp. 25-32).
8. Callister, William, D. Jr. *Materials Science and Engineering, an Introduction (7th Ed.)*, 2012; Part 001.
9. Azon. [www.azon.co/article.aspex? Article=10.6118](http://www.azon.co/article.aspex?Article=10.6118). Mechanical Properties of Low Carbon Steel of AISI. 2012; 1018.
10. Savran VI, Van Leeuwen Y, Hanlon DN, Kwakernaak C, Sloof WG, Sietsma J. Microstructural features of austenite formation in C35 and C45 alloys. Metallurgical and Materials Transactions A. 2007 May 1;38(5):946-55.
11. Prodanovic V, Militzer M, Schoir R, Kirsch H, Tacke K. *International Symposium on the Recent developments in Plates Steel*. AIST, June, Winter Park, Colorado: 2011; 317 – 322.